Supporting information

Cu-doped $La_{0.5}Sr_{0.5}CoO_{3-\delta}$ perovskite as a highly efficient and durable electrocatalyst for hydrogen evolution

Xue Yang, Fuhe Le, Zikun Zhou, Wei Jia*, Dehuo Zhou, Xianhao Chen

State Key Laboratory of Chemistry and Utilization of Carbon Based Energy Resources; Key Laboratory of Advanced Functional Materials, Autonomous Region; Institute of Applied Chemistry, College of Chemistry, Xinjiang University, Urumqi, 830046, Xinjiang, PR China.

E-mail: jia3816892@163.com

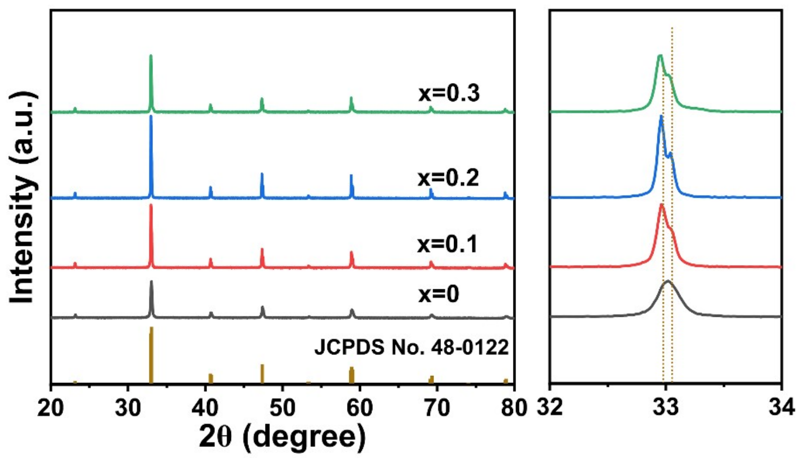

Figure S1. XRD patterns of $LSCCu_x$ (x = 0, 0.1, 0.2, 0.3) and an expanded view of the patterns in a 2θ range of 32°-34° shown on the right.

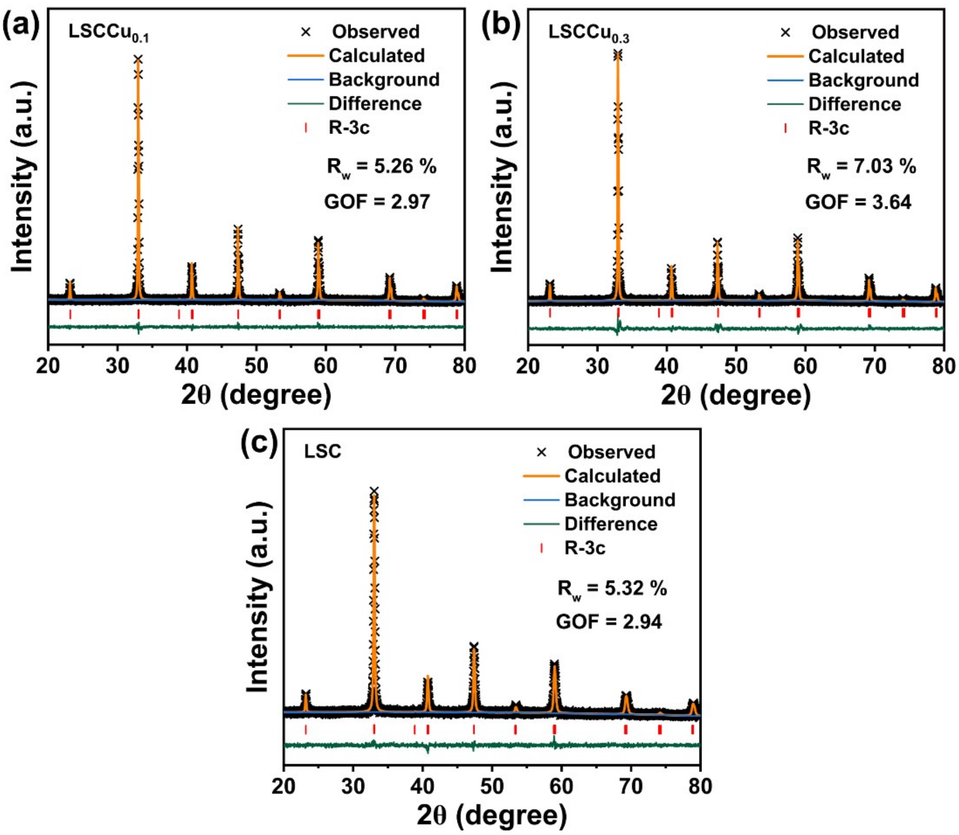

Figure S2. Rietveld refinement analyses on the XRD patterns of (a) $LSCCu_{0.1}$, (b) $LSCCu_{0.3}$, and (c) LSC.

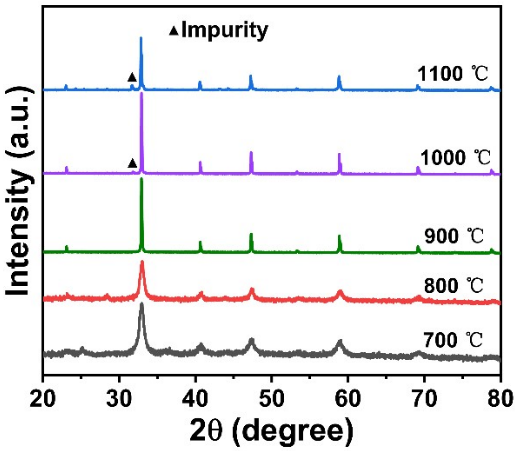

Figure S3. XRD patterns of $LSCCu_{0.2}$ prepared at 700, 800, 900, 1000, and 1100 °C, respectively.

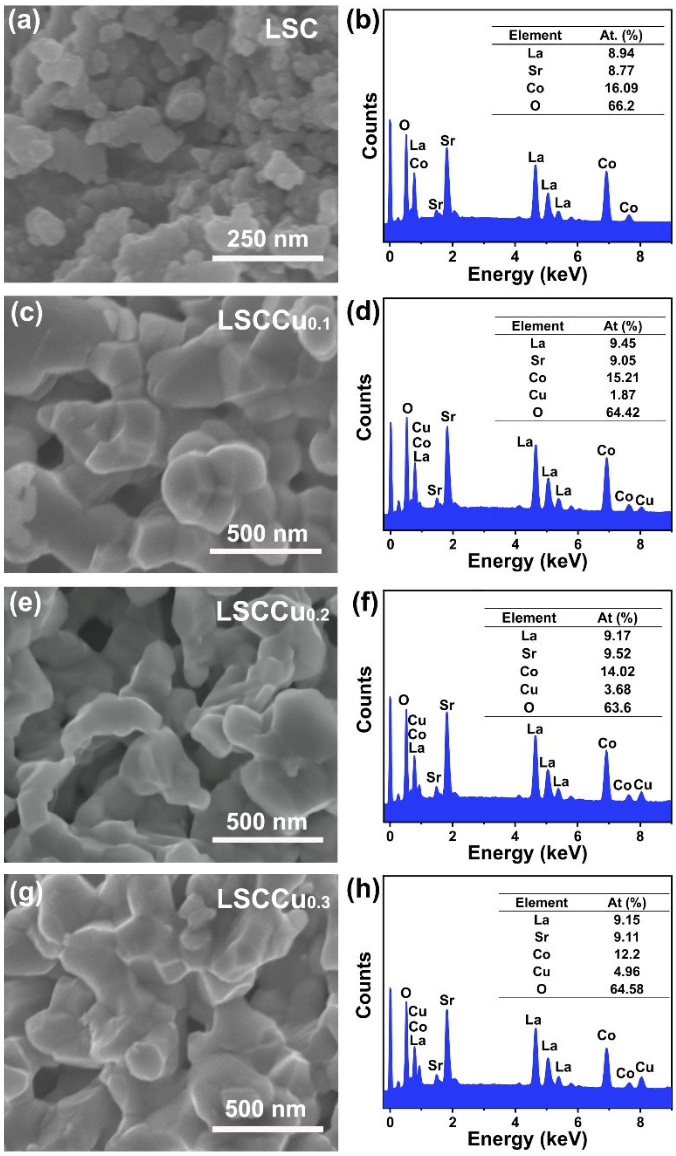

Figure S4. SEM images of (a) LSC, (c) $LSCCu_{0.1}$, (e) $LSCCu_{0.2}$, and (g) $LSCCu_{0.3}$. EDX spectra of (b) LSC, (d) $LSCCu_{0.1}$, (f) $LSCCu_{0.2}$, and (h) $LSCCu_{0.3}$.

Table S1. Element contents of the $LSCCu_x$ (x = 0, 0.1, 0.2, 0.3) determined by ICP-OES.

Catalysts	Co (wt%)	Cu (wt%)	Atomic ratio (Co/Cu)
LSC	25.49	0.00	—
$LSCCu_{0.1}$	22.97	2.81	8.87
$LSCCu_{0.2}$	21.54	5.73	4.08
$LSCCu_{0.3}$	18.06	8.65	2.26

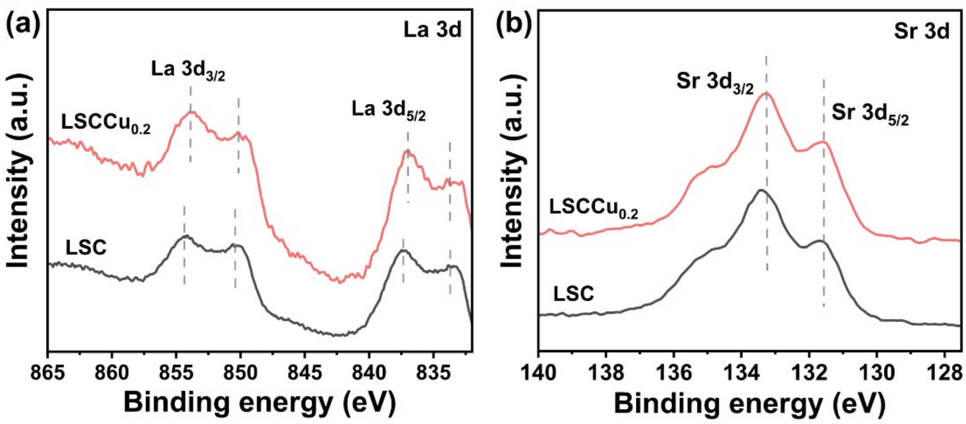

Figure S5. XPS spectra of the $LSCCu_{0.2}$ and LSC: (a) La 3d, (b) Sr 3d.

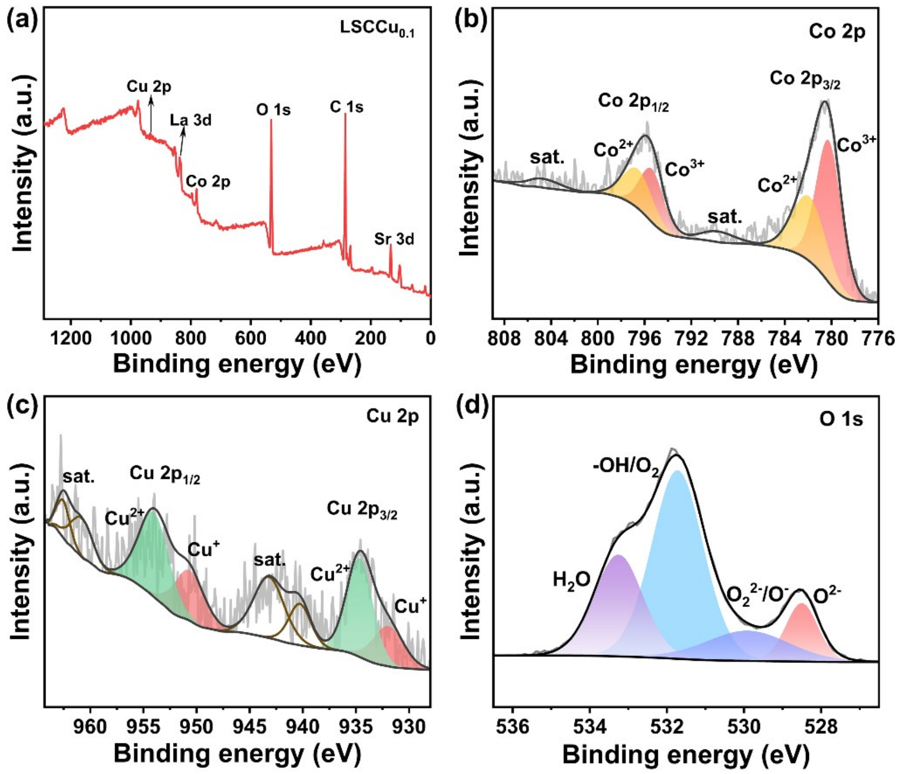

Figure S6. XPS spectra of $LSCCu_{0.1}$: (a) the survey spectrum, (b) Co 2p, (c) Cu 2p, and (d) O 1s.

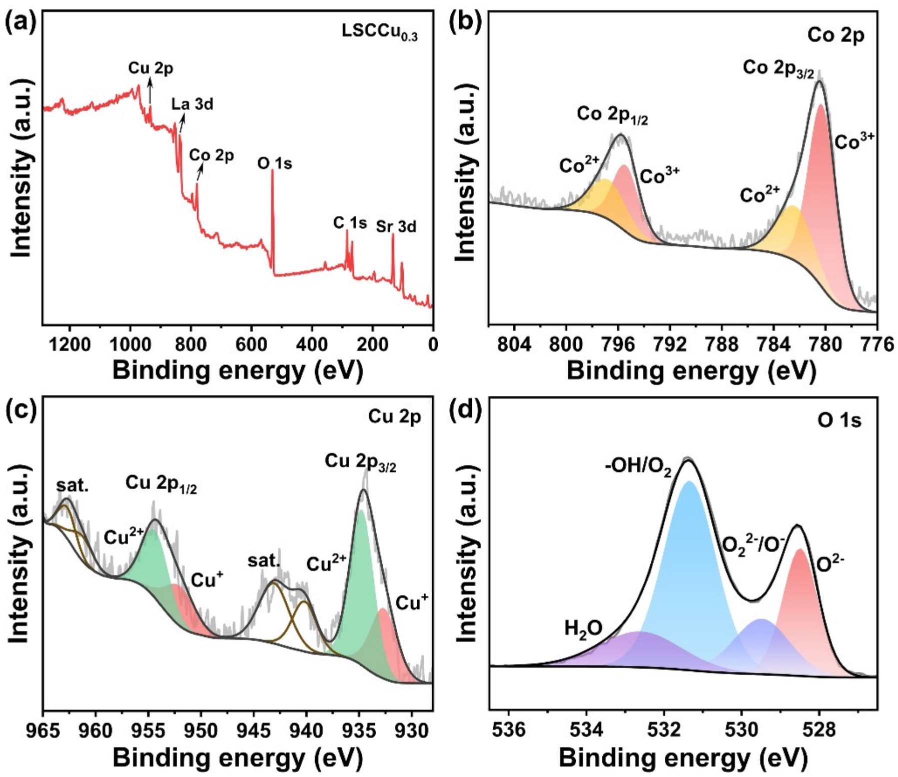

Figure S7. XPS spectra of $LSCCu_{0.3}$: (a) the survey spectrum, (b) Co 2p, (c) Cu 2p, and (d) O 1s.

Table S2. The ratios of Co^{2+} to Co^{3+} in the $LSCCu_x$ (x = 0, 0.1, 0.2, 0.3).

Catalysts	Co^{2+}/Co^{3+}
LSC	1: 1.2
$LSCCu_{0.1}$	1: 1.5
$LSCCu_{0.2}$	1: 2.7
$LSCCu_{0.3}$	1: 1.9

Table S3. The proportions of different kinds of oxygen species in $LSCCu_x$ (x = 0, 0.1, 0.2, 0.3).

Catalysts	Adsorbed H_2O/%	Adsorbed oxygen ($-OH/O_2$)/%	Highly oxidative oxygen (O_2^{2-}/O^-)/%	Lattice oxygen (O^{2-})/%
LSC	13.8	51.2	12.9	22.1
$LSCCu_{0.1}$	26.0	50.9	13.2	9.9
$LSCCu_{0.2}$	23.4	43.0	18.3	15.3
$LSCCu_{0.3}$	14.3	48.7	15.1	21.9

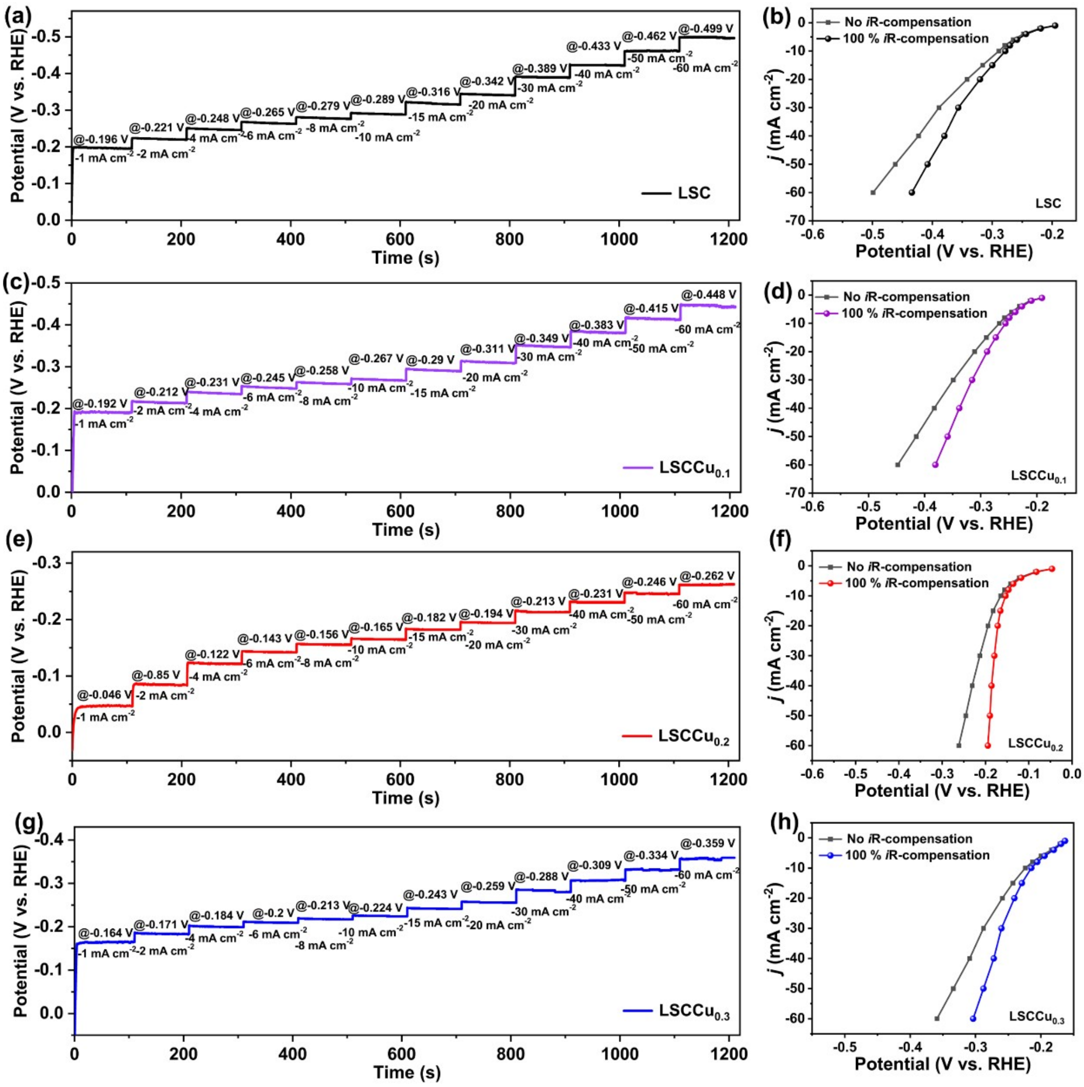

Figure S8. Chronopotentiometry responses of $LSCCu_x$ (x = 0, 0.1, 0.2, and 0.3) and corresponding plots of HER current densities with and without 100% *i*R-compensation.

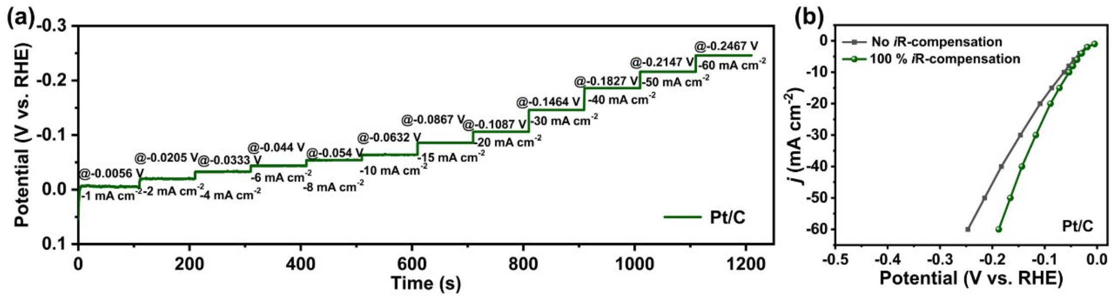

Figure S9. (a) Chronopotentiometry responses of Pt/C. (b) Plots of HER current densities with and without 100% *i*R-compensation of Pt/C.

Table S4. Comparisons of TOF of the $LSCCu_x$ (x = 0, 0.1, 0.2, 0.3).

Catalysts	TOF [H_2 s^{-1}] at η =100 mV
LSC	0.006
$LSCCu_{0.1}$	0.016
$LSCCu_{0.2}$	0.035
$LSCCu_{0.3}$	0.012

According to the reported literatures, the turnover frequency (TOF) was calculated using the following equation[1, 2]:

$$\text{TOF}=\frac{j \times A}{2 \times F \times n}$$

where j (mA cm^{-2}) represents the current densities at an overpotential of 100 mV, A is the surface area of the glassy carbon electrode (0.196 cm^{-2}), F is the Faraday constant (96485 C mol^{-1}), and n is the number of active sites (mol). The number 2 represents that two electrons are required to form one hydrogen molecule.

In this paper, Co ions are assumed to be accessible for catalyzing HER to get the value of TOF and the number of Co ions was determined by ICP-OES.

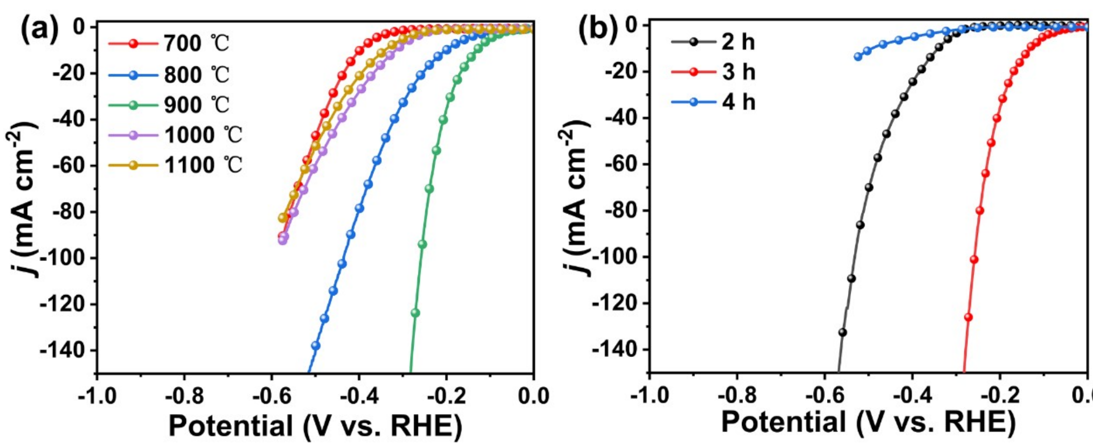

Figure S10. LSV curves of the $LSCCu_{0.2}$ prepared at different (a) calcination temperatures and (b) holding time.

Table S5. Summary of charge-transfer resistances (R_{ct}) of the LSC, $LSCCu_{0.1}$, $LSCCu_{0.2}$, and $LSCCu_{0.3}$.

Catalysts	R_{ct} (Ω)
LSC	23.6
$LSCCu_{0.1}$	20.3
$LSCCu_{0.2}$	11.1
$LSCCu_{0.3}$	15.0

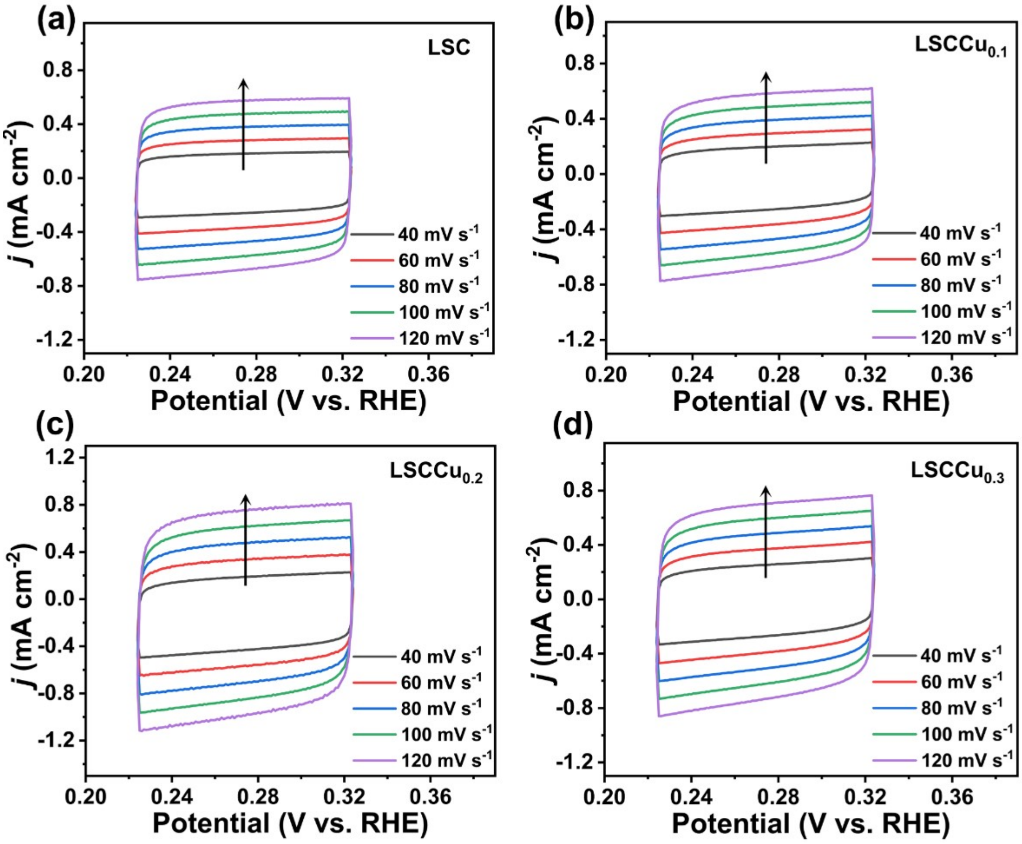

Figure S11. CV curves of (a) pristine LSC, (b) $LSCCu_{0.1}$, (c) $LSCCu_{0.2}$, and (d) $LSCCu_{0.3}$ at different scan rates in 1.0 M KOH.

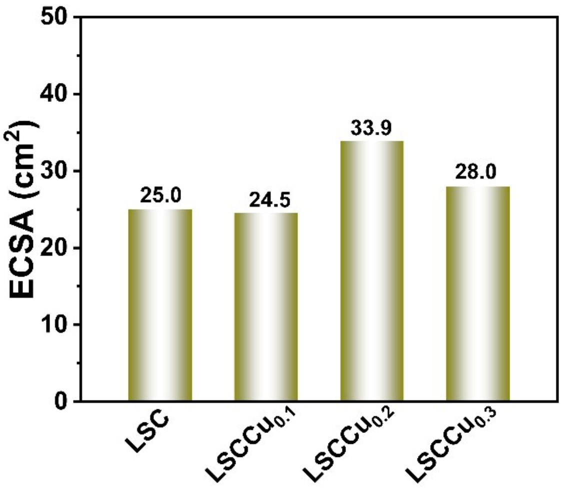

Figure S12. ECSA of the LSC, LSCCu$_{0.1}$, LSCCu$_{0.2}$, and LSCCu$_{0.3}$.

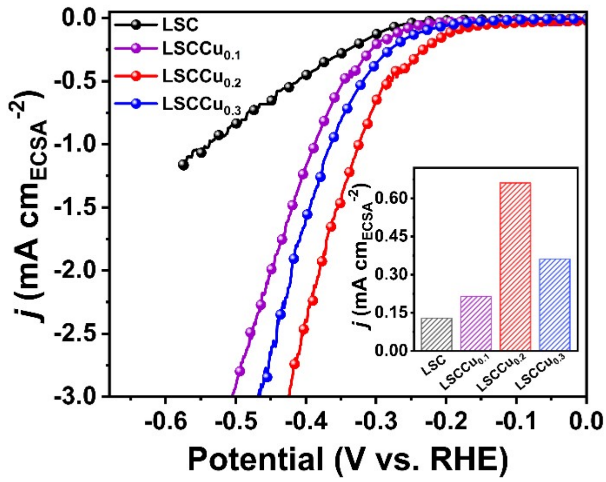

Figure S13. Specific activities (currents normalized to ECSA) of the LSC, LSCCu$_{0.1}$, LSCCu$_{0.2}$, and LSCCu$_{0.3}$ as a function of applied potential. Inset: specific activity at an overpotential of 300 mV.

Table S6. Comparisons of the HER performance of the $LSCCu_{0.2}$ with reported representative perovskite oxides in alkaline media.

Catalysts	Electrolyte	Loading ($mg_{catalyst}$ cm^{-2})	Substrate	η_{10} (mV)	Tafel slope (mV dec^{-1})	Reference
$La_{0.5}Sr_{0.5}Co_{0.8}Cu_{0.2}O_{3-\delta}$	1 M KOH	0.255	GC	**154**	120	**This work**
$SrIrO_3$	0.1 M KOH	0.232	GC	139	49	Chem. Mater., 2020, 32, 4509-4517
$La_{0.5}Ba_{0.2}Sr_{0.2}Ca_{0.1}Co_{0.8}Fe_{0.2}O_{3-\delta}$	1 M KOH	0.255	GC	~190	59	Adv. Energy Mater., 2017, 7, 1700666
$La_{0.5}Ba_{0.25}Sr_{0.25}CoO_{3-\delta}$	1 M KOH	0.157	GC	~220	51	Chem, 2018, 4, 2902-2916
$Pr_{0.5}(Ba_{0.5}Sr_{0.5})_{0.5}Co_{0.8}Fe_{0.2}O_{3-\delta}$	1 M KOH	0.232	GC	237	45	Adv. Mater., 2016, 28, 6442-6448
$(Gd_{0.5}La_{0.5})BaCo_2O_{5.5+\delta}$	1 M KOH	0.232	GC	240	27.6	Nat. Commun., 2019, 10, 3755
$PrBaCo_2O_{5.8}$	1 M KOH	0.255	GC	240	61	Mater. Chem. Front., 2020, 4, 1519-1529
$PrBaCo_2O_{5+\delta}$-1100	0.1 M KOH	0.398	GC	245	89	J. Power Sources, 2019, 427, 194-200
N-doped $Sr_2Fe_{1.5}Mo_{0.5}O_{6-\delta}$-450	1 M KOH	1.5	CC	251	138	Mater. Today Energy, 2021, 20, 100695
$SrNb_{0.1}Co_{0.7}Fe_{0.2}O_{3-\delta}$	0.1 M KOH	0.232	GC	262	134	Adv. Energy Mater., 2017, 7, 1602122
$La_{0.1}Sr_{0.9}Fe_{0.5}Co_{0.475}P_{0.025}O_{3-\delta}$	1 M KOH	0.232	GC	280	119	ACS Materials Lett., 2021, 3, 1258-1265
$NdBaMn_2O_{5.5}$	1 M KOH	~0.4	GC	290	87	ACS Catal., 2018, 8, 364-371
$LaCo_{0.94}Pt_{0.06}O_{3-\delta}$	0.1 M KOH	0.3	CP	294	148	RSC Adv., 2019, 9, 35646-35654
$Sr_{0.95}Nb_{0.1}Co_{0.7}Ni_{0.2}O_{3-\delta}$	1 M KOH	1	CP	299	80	J. Mater. Chem. A, 2019,7, 19453-19464
$La_{0.96}Ce_{0.04}CoO_{3-\delta}$	1 M KOH	0.734	GC	305	144	Nanoscale, 2021, 13, 9952
$SrCo_{0.7}Fe_{0.25}Mo_{0.05}O_{3-\delta}$	1 M KOH	0.362	GC	323	94	Electrochim. Acta, 2019, 312, 128-136
$SrTi_{0.1}Fe_{0.85}Ni_{0.05}O_{3-\delta}$/CNT-700	0.1 M KOH	~0.724	GC	340	166	Electrochim. Acta, 2018, 286, 47-54
$Ba_{0.5}Sr_{0.5}Co_{0.8}Fe_{0.2}O_{3-\delta}$	1 M KOH	0.232	GC	342	75	Adv. Mater., 2016, 28, 6442-6448
$LaFe_{0.8}Co_{0.2}O_{3-\delta}$	1 M KOH	0.232	GC	~400	113	Adv. Mater. Interfaces, 2019, 6, 1801317

$La_{0.5}Sr_{0.5}CoO_{3-\delta}$	1 M KOH	0.385	GC	~420	95	Nat. Commun., 2019, 10, 1723
Ca_2FeRuO_6	1 M KOH	---	GC	420	---	ACS Appl. Energy Mater., 2021, 4, 1323-1334
$La_{0.8}Sr_{0.2}Cr_{0.69}Ni_{0.31}O_{3-\delta}$	0.1 M KOH	0.401	GC	447	116	Electrochim. Acta, 2019, 318, 120-129

In the table above, some abbreviations stand for:

η_{10}: The overpotential required to reach a current density of 10 mA cm^{-2}.

GC: Glassy carbon.

CC: Carbon cloth.

CP: Carbon paper.

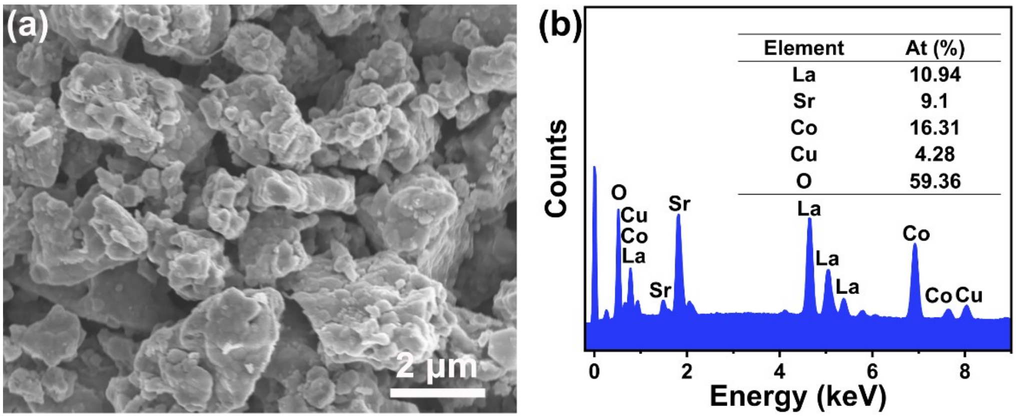

Figure S14. (a) SEM image and (b) EDX spectrum of the $LSCCu_{0.2}$ after HER.

Table S7. The content of the metal ions in the electrolyte after HER determined by ICP-OES.

elements	La	Sr	Co	Cu
mg/L	0	0.18	0	0

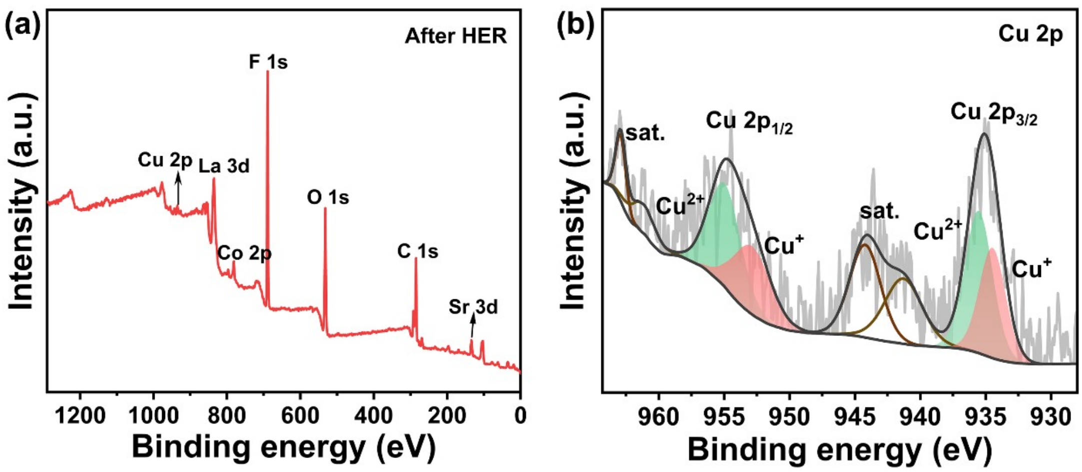

Figure S15. (a) XPS survey scan and (b) Cu 2p of the $LSCCu_{0.2}$ after HER.

References

1. Y. Liu, S. Liu, Y. Wang, Q. Zhang, L. Gu, S. Zhao, D. Xu, Y. Li, J. Bao and Z. Dai, *J. Am. Chem. Soc.*, 2018, **140**, 2731-2734.
2. D. Xue, J. Cheng, P. Yuan, B.-A. Lu, H. Xia, C.-C. Yang, C.-L. Dong, H. Zhang, F. Shi, S.-C. Mu, J.-S. Hu, S.-G. Sun and J.-N. Zhang, *Adv. Funct. Mater.*, 2022, **32**, 2113191.